scientific reports

Check for updates

OPEN

Anterior cruciate ligament reconstruction in a translational model in sheep using biointegrative mineral fiber reinforced screws

Brian J. Cole[1]✉, Jeremiah T. Easley[2], Abraham Nyska[3] & Serge Rousselle[4]

Anterior cruciate ligament reconstruction (ACLR) is one of the more common procedures performed worldwide and perhaps the most widely studied construct in orthopedic literature. Interference screws are reliable and frequently used for ligament reconstruction, providing rigid fixation and facilitates graft incorporation allowing for the physiologic loads of early rehabilitation. The purpose of this study was to determine the bio-integration profile and quality of soft tissue graft when using mineral fiber-reinforced screws in an ACLR interference model. Nine sheep underwent ACLR using harvested autologous tendon graft fixated with 4.75 mm screws made of continuous mineral fibers. Histopathology and imaging evaluation at 28, 52, 104, 132-weeks (W) demonstrated mesenchymal tissue ingrowth into implant wall at 28 W, which increased at 52 W and peaked at 104 W. At 132 W, implants fully replaced by newly remodeled bone. Graft cellularity was evident at 28 W and continued to increase through 132 W as the tendon ossified at sites of bone contact. Pro-healing M2-macrophages and giant cells remained infrequent, with minor increases between 52 W and 104 W, attributed to expected phagocytic response. Pro-inflammatory cells (i.e., M1-macrophages, polymorphonuclears) were absent through the entire study course. In conclusion, bio-integrative screws provide secure soft tissue fixation with replacement by bone demonstrating graft cellularization over time.

Orthopedic injuries commonly involve damage to soft tissues such as tendons and ligaments. Reconstruction procedures using grafts require tissue attachment to bone[1,2]. Soft tissue fixation is widely used to repair injuries to the knee, shoulder, elbow, as well as foot and ankle injuries[2–6]. The quality of fixation is particularly important as graft integration with hard tissues is essential for early initiation of rehabilitation and late tissue remodeling and incorporation[7,8].

Ligament reconstruction using a graft undergoes four phases of integration. First, an inflammatory response occurs with ischemic necrosis. Following this, cell recruitment and chronic inflammation occurs followed by revascularization, cell proliferation and finally, collagen remodeling[9,10].

Bone ingrowth plays an important role in the graft-to-bone fixation, and thus supports the healing process of the graft[8]. Different biological agents, such as calcium-phosphate, magnesium-based bone adhesive, hyperbaric oxygen, transforming growth factor-beta 1 (TGFβ-1) as well as mesenchymal stem cells, have been found to increase bone ingrowth into tendon grafts placed in a bone tunnel by their activation of cell differentiation signaling pathways[11,12].

The enthesis is the site where the soft tissue (tendon or ligament) inserts onto bone and where stress concentration occurs[13,14]. Numerous fixation methods address the soft tissue to bone repair site[2,15–17]. The main function of these devices is to secure soft tissue at the appropriate bony site until physiologic healing occurs[18]. Interference screws (IS) are a reliable and frequently used method for graft fixation as they provide rigid and direct attachment to bone facilitating osseous healing and early rehabilitation[19–22].

Metal IS are generally inexpensive and easy to insert, provide high failure loads, and historically have afforded relatively positive clinical outcomes[18,20,23]. Nonetheless, metallic screws carry inherent limitations including graft laceration during insertion, interference with surgical revision, and lead to substantial artifact on post-implantation MRI assessment with a general desire to avoid radio-dense metal where possible[24,25]. Bioabsorbable polymer based IS are an alternative method for soft tissue or bone fixation. They can decrease

[1]Department of Orthopaedic Surgery, Rush University Medical Center, Chicago, IL, USA. [2]Preclinical Surgical Research Laboratory, Department of Clinical Sciences, Colorado State University, Fort Collins, CO, USA. [3]Toxicologic Pathology , Tel Aviv University, Tel Aviv, Israel. [4]StageBio, Frederick, MD, USA. ✉email: Brian.Cole@rushortho.com

stress shielding due to their ability to gradually transfer loads as they degrade, they are unlikely to cause graft damage during insertion and do not distort post-operative imaging assessment[18,26,27]. The most commonly used polymers for soft tissue fixation are polyglycolic acid (PGA), poly-L-lactic acid (PLLA), poly-D-lactic acid (PDLA) and poly lactide-co-glycolide (PLGA), with or without different ratios of mineral compounds, such as hydroxyapatite (HA) and β-tricalcium phosphate (β-TCP). These implants, however, pose their own inherent risks which can be divided into "early" and "late" complications. The "early" shortcomings, experienced around the time of surgery and include intraoperative screw breakage, loss of fixation, graft slippage, and screw migration[18,28]. The "late" complications are usually associated with an imbalanced degradation response reflected by inflammatory reactions leading to accelerated or incomplete absorption, joint effusion, bone tunnel widening and encapsulation[18,24,28–31]. Additional reported material-related complications are cyst or abscess formation, intraarticular granulomas and adverse foreign body reactions which might result in osteolysis, synovitis and rarely, systematic allergic response[20,29].

The bio-integrative screw used in the current study is composed of a unique continuous mineral fiber matrix made of elements found in native bone, bound together with PLDLA [poly (L-lactide-co- D, L-lactide). The implant material is designed to encourage a paced and gradual bio-integrative response, aiming to eliminate the risks and complications related to acute degradation which may lead to adverse inflammation. The mineral component is known to promote bone growth and regeneration[32] and balances decreasing pH levels as the polymer is being absorbed[33,34]. Gradual and balanced elimination of the mineral fiber-reinforced implant has been demonstrated in various in vivo bone implantation studies with complete bio-integration at 104 weeks and no adverse inflammation[35].

The purpose of this in vivo study was to evaluate the safety and bio-integration profile of mineral fiber-reinforced screws into bone, and evaluate quality of soft tissue graft involved in ACLR interference model.

Methods

Study device

The bio-integrative implants used in this study (OSSIO*fiber*®, OSSIO Ltd., Caesarea, Israel) are 4.75 mm screws made of continuous reinforcing mineral fibers (50% w/w ratio) comprised of elements found in native bone (SiO_2, Na_2O, CaO, MgO, B_2O_3, and P_2O_5), bound together by PLDLA (70:30 L: DL ratio).

Animals, surgical procedure, and postoperative care

This in vivo study was conducted at the Preclinical Surgical Research Laboratory at Colorado State University. Animal care, surgical procedures and all experimental protocols were approved and performed in accordance with the local Research Unit Ethics committee- Colorado State University IACUC (Institutional Animal Care and Use Committee) protocol KP #1747. All methods were carried out in accordance with relevant guidelines and regulations. The study is reported in accordance with ARRIVE guidelines.

Nine female sheep (*Ovis aries*) (Source: USDA approved vendor, K&S Livestock, Fort Collins, CO) underwent ACL simulated reconstruction of the right stifle using an all soft-tissue autograft (Fig. 1a-c). Anesthesia was induced with ketamine (3.3 mg/kg) and midazolam (0.1 mg/kg) intravenous (IV) and maintained with isoflurane (1.5-3%). The animals were placed in dorsal recumbency, wool was clipped over the right stifle and entire distal limb, and the skin was prepped for aseptic surgery.

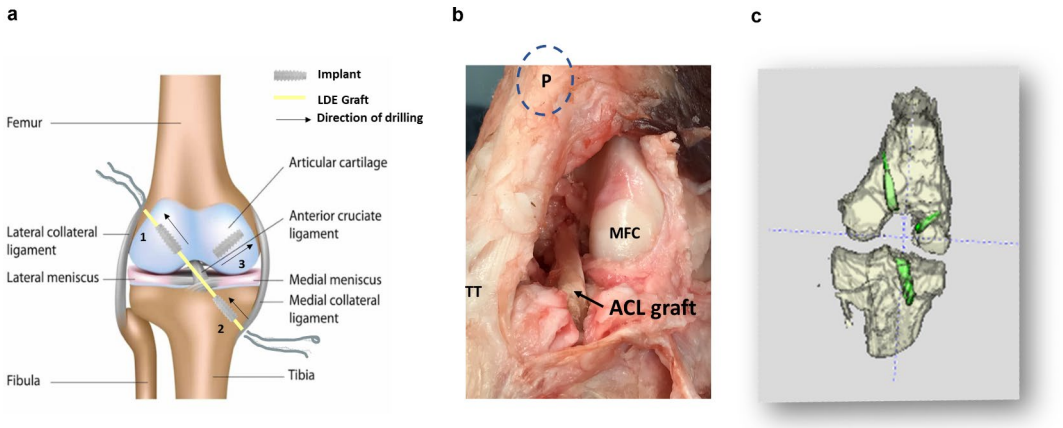

Fig. 1. Ovine in-vivo bone and soft tissue interference model. Anatomical illustration of the sheep knee, Sites 1 & 2 represent tendon graft interference implantation in the femur and tibia respectively. Site 3 – screw implanted directly in bone (**a**). Intraoperative (time zero) image of the ACL graft inserted into femoral and tibial drill tunnels P = Patella. TT = Tibial Tuberosity. MFC = Middle Femoral Condyle (**b**). MRI coronal view of the implanted knee joint (**c**).

Preparation of the tendon graft
A small incision was made along the lateral edge of the right metatarsal bone and the lateral edge of the distal tibia. The Lateral Digital Extensor (LDE) tendon was located at both sites, transected distally, and pulled through the subcutaneous tissue through the proximal incision. Using a tendon stripper, the LDE was transected yielding ~ 130 mm tendon graft, doubled over and placed into a graft jig. The free end of the graft was sutured utilizing a running interlocking suture configuration. The LDE graft was then measured for length and diameter using a graft sizing tool. The tendon graft was covered with saline-soaked gauze until the implantation site was prepared.

Intra-articular implant placement
A medial mini-arthrotomy was performed from the tibial plateau to the vastus medialis. The fat pad was removed along with the ligamentum mucosum in order to visualize the ACL.

ACL simulated reconstruction procedure The ACL insertion was located on the tibia and femur. Pilot holes for the screws interfacing with soft tissue grafts were planned in a natural loaded position. A 2.4 mm guide pin was drilled freehand anterior to the femoral insertion of the ACL footprint in an inside-outside fashion. An appropriately sized reamer (based on the ACL graft measured diameter) was utilized to over-drill the guide pin to a 20 mm depth. Using a slotted beath pin, a passing suture (#1 monofilament) was inserted into the femoral socket. To create the tibial tunnel, the ACL tibial insertion was located and a 2.4 mm guide pin was drilled from outside-in anterior to insertion site, followed by over-drilling with an appropriately sized reamer (based on ACL graft diameter). Using a slotted beath pin, a passing suture (#1 monofilament) was inserted into the tibial tunnel. The LDE graft was then pulled into the femoral and tibial tunnels using the preplaced passing sutures. Once fully seated and tensioned within the femoral tunnel, a 4.75 mm screw was inserted adjacent to the graft in an inside-out fashion. The stifle was then flexed to permit an outside-in insertion of a second 4.75 mm screw adjacent to the graft within the tibial tunnel.

Direct implantation in bone Lastly, a third 4.75 mm screw was implanted into the bone of the medial intercondylar arch in an inside-out fashion. A 2.4 mm guide pin was drilled through followed by over-drilling using a 4.5 mm reamer. The defect was irrigated thoroughly and a 4.75 mm screw was implanted into the bone in isolation, without an adjacent soft tissue graft.

Routine closure of the joint capsule and fascia was performed using #0 absorbable suture followed by subcutaneous tissue with #2-0 absorbable suture and skin with #2-0 non-absorbable suture. Animals received antibiotics (Penicillin G (procaine) (22,000u/kg) SQ (Subcutaneous)) starting one day preoperatively and for two days postoperatively.

Surgical after-care
Analgesics were received preoperatively (Phenylbutazone (/Bute), (1 gram) PO (Oral administration)) and (Fentanyl patch, Transdermal) (150 mcg/hr) and once daily postoperatively for up to 6 days.

The sheep were housed in the facility barn for a minimum of 4 weeks postoperatively. Animals were then moved out to pasture for the remainder of the study period. Sheep were monitored daily throughout the study period for any signs of adverse events or discomfort by evaluating pain, lameness, incisional sites, and ambulatory function as well as general health status. If an animal was noted to have abnormal clinical findings during routine daily monitoring, a complete physical examination was performed by a veterinarian and a diagnostic and therapeutic plan was implemented.

Imaging

Radiographic imaging
Anterior-posterior (AP) and Lateral radiographic views of the right knee were performed for all animals immediately post-operatively and on the day of sacrifice.

Magnetic resonance imaging (MRI)
Sheep were placed under general anesthesia to undergo MR imaging of a single limb (R hind limb) at 12, 28, 52, 104 and 130 weeks. Sagittal, transverse, and/or coronal sections were obtained with a series of sequences.

Sample collection

Animals were humanely euthanized by intravenous overdose of pentobarbitone sodium (88 mg/kg), in accordance with the American Veterinary Medical Association (AVMA) guidelines, at 28 ($n=3$), 52 ($n=2$), 104 ($n=2$) and 132 weeks ($n=2$). The right stifles were collected, and the soft tissue surrounding the joints was dissected to isolate the joints. Specimens were fixed in 10% neutral buffered formalin and stored at room temperature. Downstream draining lymph nodes (popliteal and superficial inguinal) were also collected and shipped to the pathology test site (StageBio Pathology, Frederick, Maryland, USA).

Bone and tissue sample preparation

Formalin-fixed stifles were disarticulated, and soft tissues were removed from the outer cortical surfaces to expose the healed drill sites. The native cruciate ligaments were transected for disarticulation but otherwise maintained. The three implantation sites were isolated using a diamond blade bone saw, processed through a graded series of ethyl alcohol and embedded in methyl methacrylate. The blocks were sectioned in predefined multiple levels, using a diamond band saw. Two slides were produced at each level; one was stained with hematoxylin and eosin (H&E), and the other was stained with Stevenel's blue.

Histopathology

Two types of implantations were histologically evaluated in the current study; Sites 1 & 2 demonstrate implantation in an interference fashion with bone- implant-tendon graft interface, while site 3 represents direct bone-to-implant interface (Figs. 1a and 2a, b).

Each slide was semi-quantitatively graded according to ISO 10993-6 Annex E:

(1) Amount of residual polymer and mineral fibers remaining compared to baseline (none (0), 1–25% (1), 26–50% (2), 51–75% (3), and 76–100% (4)).
(2) Material bioabsorption based on amount of residual polymer and mineral fibers, recorded as no absorption (76–100% of polymer/ mineral remaining (0)), slight absorption (51–75% of polymer/mineral remaining (1)), moderate absorption (26–50% of polymer/mineral remaining (2)), marked absorption (1–25% of polymer/mineral remaining (3)), or complete absorption (no polymer/mineral remaining (4)).
(3) New bone formation and cellular/tissue ingrowth into the implant wall: Not present (0), Minimal (1) Mild (2) Moderate (3) or Marked (4).
(4) Slides stained with H&E were also evaluated for: overall inflammation (i.e., inflammatory macrophages (M1-like macrophages; pro-inflammatory); polymorphonuclear cells, lymphocytes, and plasma cells; phagocytic macrophages (M2-like macrophages; pro-healing (anti-inflammatory)) and giant cells.

Necrosis, fibrosis and neovascularization were semi-quantitatively graded.

Tendon graft evaluation

Graft cellularity and graft ossification as measures of tendon-bone tunnel integration were scored at the graft ends at sites 1&2 (Not present (0); Minimal (1); Mild (2); Moderate (3); or Marked/Severe (4)).

Data analyses

All quantified data were described as means and standard deviations of scores at each time point. An unpaired two tailed Student's t test was used for the analysis of the various parameters. Values of 0.05 or less were considered statistically significant. Clinical observations were descriptive in nature.

Results

Intraoperative performance

All surgical procedures were consistently performed across all animals and completed successfully utilizing the established ovine model (Fig. 1a,b). Implantation of the bio-integrative screws did not require pre-tapping of the drilled pilot holes and all screws were implanted and seated well into untapped bone tunnels in both the femur and tibia with a single initial attempt at screw placement. No intraoperative thread stripping, screw breakages or cutting of the tendon graft were reported. No other intraoperative technical complications arose.

Clinical observations

Operated animals and all surgical sites were regularly examined, with no reported gait abnormalities after the initial post-operative period nor was there evidence of local soft tissue reaction observed in any of the animals at any time point. Incidences of lameness during the immediate postoperative recovery period were considered as an anticipated finding and resolved following analgesics and after the initial phase of recovery prior to the transition to pasture. No animals were withdrawn from the study due to morbid conditions, unexpected death, or were euthanized prior to study completion.

Gross morphology

No adverse findings were noted upon gross examination at necropsy. Healing features appeared favorable in all animals irrespective of the sacrifice timepoint.

Histopathology

Tissue ingrowth & new bone formation

A moderate amount of new bone formation along and around the implant was evident as early as 28 W. Implantation sites demonstrated score of 1 (±0) cellular ingrowth at the implant-bone interface, characterized

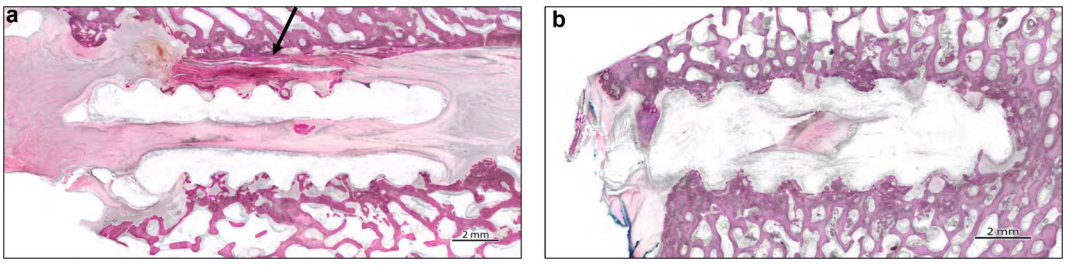

Fig. 2. Histology images of the two types of implantation sites (H&E). Representative histology image of interference screw implantation with tendon graft (black arrow) (site 1) at 28 W, longitudinal section (**a**). Direct implantation in bone (site 3) at 28 W, longitudinal section (**b**).

by ingrowth of fibroblasts, macrophages and occasional new bone formation within small implant matrix cavities (Fig. 3a,e). The tissue ingrowth increased at 52 W (1.57 ± 0.23, Fig. 3b,e). As the bio-integration response progressed (104 W), cellular ingrowth increased significantly, reflected by a score of 4 (± 0) (Fig. 3c,e). At 104 and 132 W the implant was substantially replaced by new bone formation, irrespective of whether implanted in an interference fashion or directly in bone (Fig. 3c,d). New trabecular bone formation at 132 W was indicative of advanced tissue replacement and healing. At this time point the newly formed bone was already matured.

The evaluation of new bone formation was descriptive in nature, as the soft tissue interference model made it challenging to isolate implant-bone interface in the presence of the tendon graft to otherwise perform a quantitative assessment.

Bioabsorption

Early stage bioabsorption was evident as early as 28 W (grade score 0.78 ± 0.67) with minimal macrophagic activity in the form of large, monomorphic macrophages and giant cells along the implant surface (Fig. 4a). At 52 W, a score of 1.00 ± 0.76 was characterized by minimal to mild phagocytic activity with infiltrating macrophages and giant cells mainly evident at the implant-host interface, occasionally extending to mid-implant wall thickness.

Implant bioabsorption was nearly complete by 104 W (score of 4.00 ± 0.00), evidenced by only a few small islands of polymer remaining, while mineral fibers were completely absent at this late study timepoint. Residual phagocytic activity was still evident, characterized by a small number of clusters of infiltrating macrophages and giant cells within the tract of the implant site. At 132 W, the screw was completely replaced by normal bone architecture without cystic formation and without residual phagocytic macrophages observed (Fig. 4d).

Overall inflammation and cell types

At 28 W, no or very few aggregates of pro-healing cells were observed along the extramedullary region of the implants. Large phagocytic macrophages with abundant cytoplasm in monomorphic aggregates (i.e., consistent with M2-like macrophages)[36] were evident primarily in conjunction with early polymer absorption (Fig. 4a). Low numbers of multinucleated giant cells consistent with early phagocytic response were evident along the implant surface. Phagocytic macrophages and giant cell infiltrates remained infrequent through all time points, with minor increases (1.60 ± 0.70) between 52 and 104 W attributed to phagocytic activity. Lymphocytes, plasma cells and polymorphonuclear cells were absent at all timepoints (Fig. 4a-d).

Cellular response in the presence of the implant and graft construct was similar within the intramedullary cancellous region and the extramedullary region as described above, at 28 W, 52 W, 104 W and 132 W.

Tendon graft viability

At 28 W the tendon graft showed cellularity score of 2.83 ± 0.41 (Fig. 5a,b,d) with some expected cell loss upon graft collection and surgical implantation. By 104 W, increased tissue integration and tendon anchoring was observed along the graft-tendon interface, with increasing graft cellularity (score 3.44 ± 0.53) (Fig. 5c,d) and areas of ossification representative of tendon integration into host bone (Fig. 6a). No differences were noted with respect to implantation site location (femoral vs. tibial). At 132 W, the graft showed optimal bone integration with areas that were largely ossified (score 3.29 ± 0.34) primarily deeper in the bone tunnel (Fig. 6b-d). Cellular infiltration scores trending downward (1.22 ± 1.39) in direct correlation with graft ossification in areas of graft-bone contact.

Necrosis, fibrosis, and neovascularization

No necrosis, fibrinous exudates or tissue degradation were observed in the host tissue around the implants or grafts at any time point. The dominant tissue response at sites 1 & 2 in the presence of tendon-graft consisted of fibrous connective tissue healing with varying degrees of collagen deposition along the implant. Site 3 was

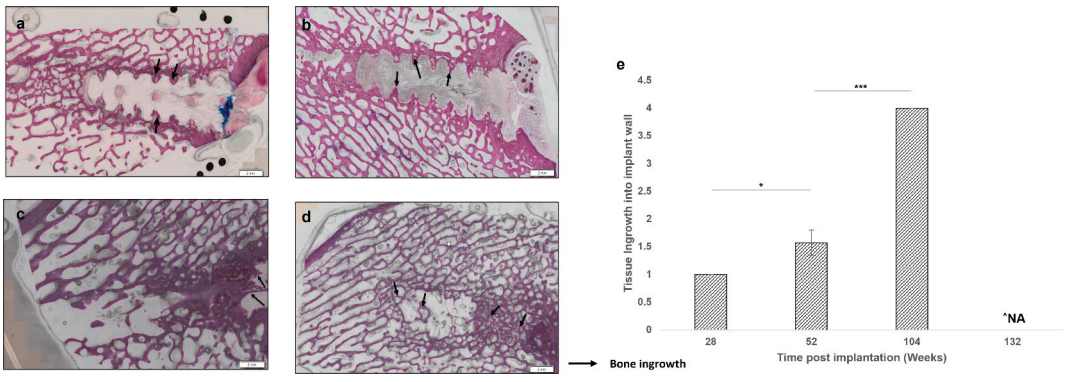

Fig. 3. Tissue ingrowth into implant wall. Representative histology images (H&E) of site 3 at 28 W (**a**), 52 W (**b**), 104 W (**c**) and 132 W (**d**) and average ± SE tissue ingrowth scores presented as evaluated from histology slides (**e**). P values considered statistically significant when $p < 0.05$ (*), 0.01 (**), 0.001 (***). ^ No implant material remaining.

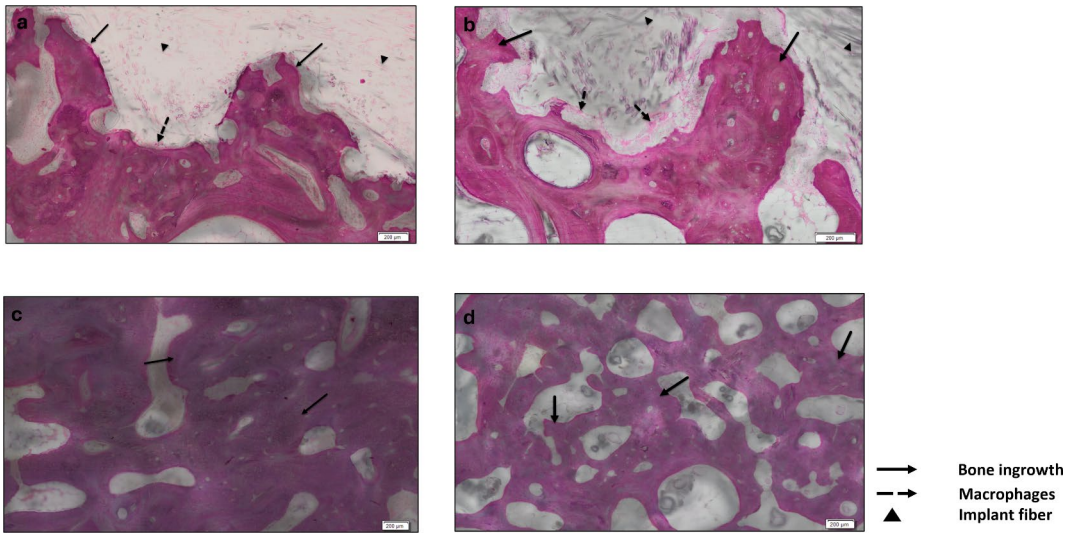

Fig. 4. Phagocytic macrophage activity. Representative histology images (H&E) of site 3 at 28 W (**a**), 52 W (**b**), 104 W (**c**) and 132 W (**d**). Macrophage activity Score of 1 noted at different study timepoints. This Bio-integration response advances as the phagocytic cells are clearing the polymer content, while the tissue and bone ingrowth progresses.

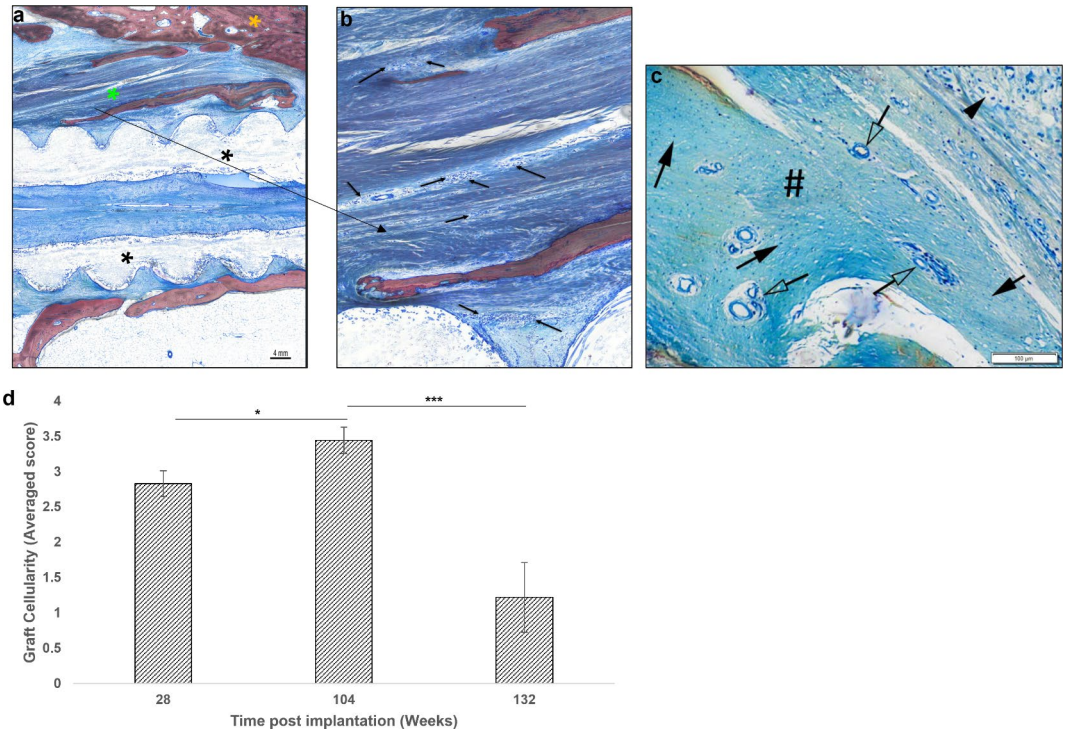

Fig. 5. Tendon graft cellularity. Representative histology images (SB) of site 1 at 28 W (**a**,**b**). (**a**) Low magnification: Black asterisks = bio-integrative screw; Green asterisk = Tendon graft; Orange asterisk = trabecular bone. (**b**) Higher magnification: Black arrows = viable fibroblasts. Site 2 at 104 W (**c**): Tendon graft (#) showing recellularization (solid arrows) and neovascularization (clear arrows). Tendon graft cellularity graph (**d**): Averages ± SE scores evaluated from histology slides. P values considered statistically significant when $p < 0.05$ (*), 0.01 (**), 0.001 (***).

characterized by direct bone remodeling and replacement. Neovascularization was slight to mild at 28 W, with occasional small groups of capillaries observed at 52 W, 104 W (Fig. 5c), and 132 W.

Lymph nodes

Minimal, non-adverse ceroid-laden macrophages were observed in draining lymph nodes (popliteal and/or superficial inguinal) which was an anticipated finding for the animal model. There were no adverse effects in downstream lymph node noted and there were no changes attributable to the implants at any time periods.

Discussion

Damage to soft tissues, including the anterior cruciate ligament (ACL), constitute a significant area of interest in orthopedics and sport medicine. Treatment of these injuries utilizing tendon or tendon bone constructs has some inherent limitations related to graft fixation. This is commonly achieved with interference screw (IS) fixation with specific design considerations[37]. The main function of an IS in ACL repair is to secure graft tissue to the appropriate bony site and hold it in place until the graft incorporates within the bone tunnel and physiologic healing is achieved[18,38]. Metal IS have been commonly used for many years and provide high initial fixation strength with advantageous load-to-failure mechanics. Nevertheless, distortion on postoperative MRI assessment as well as the need for hardware removal at the time of revision surgery and a general desire to avoid permanent hardware have led to the utilization of their bioabsorbable counterparts[25,39,40]. These polymer-based implants, however, may present other considerable limitations or concerns such as intra- and postoperative screw breakage or migration and material-related adverse tissue responses including cyst formation and synovitis.

Bioabsorbable devices are designed to degrade overtime. Any mismatch between implant absorption and healing kinetics may result in adverse inflammation which further inhibits healing[36]. Hovis et al. reported the histological results of PGA screws used for fixation of medial malleolar fractures, of which 8 of 16 patients developed implant-related inflammatory reactions at 3 to 4 months[41]. Walton et al. described the lengthy degradation of PLLA interference screws 3 years and more following ACL reconstruction in sheep. Their study documented the occurrence of a second phase of cellular activity characteristic of a long term, localized chronic inflammatory reaction[42]. Seino et al. described a case of rotational acetabular osteotomy fixation for acetabular dysplasia using PLLA screws. Histological results demonstrated acute inflammation 19 months postop, leading to the need for debridement surgery[43]. Several case studies followed radiographic and histological results of ACL reconstruction with a hamstring autograft or allograft using PLLA screws. Their findings indicated 5% of multiloculated pretibial cysts with histiocytic infiltrate around the PLLA debris with surrounding acellular cystic material 2–3 years following implantation[44]. These findings can appear years following initial implant

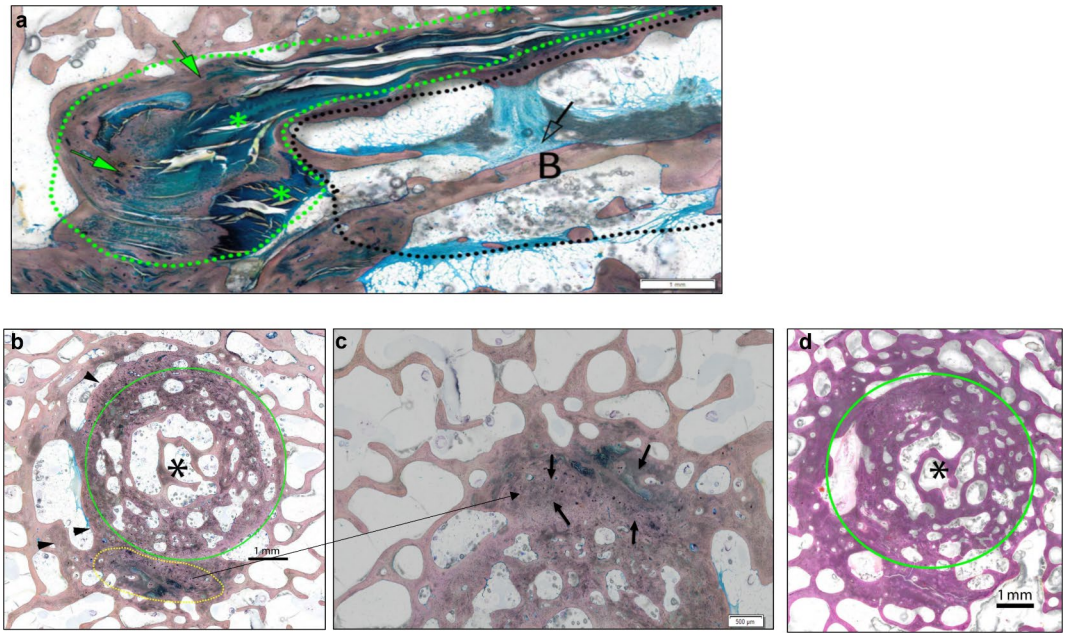

Fig. 6. Tendon graft ossification & implant site bio-integration. Representative histology images (SB) of graft site 1 at 104 W in longitudinal section (**a**): Black dotted line = implantation tract of the implant showing no residual implant material remaining and regeneration of trabecular bone (B), with minimal residual phagocytic response (clear arrow). Green dotted line = recellularized tendon graft (green asterisks) with areas of ossification (green arrows) representative of tendon anchoring in host bone. Graft site 2 in cross section at 132 W (**b**) and higher magnification of the tendon graft (**c**): Green circle = Implantation site showing complete bio-integration and replacement by newly remodeled trabecular bone (black asterisks); New bone remodeling also shown along the edges of the implant site (black arrowheads). Yellow dotted line = area of tendon graft showing integration within new bone and permanent anchoring of the graft (= ossification, black arrows). 132 W graft site in cross section (H&E) (**d**): Green circle = drill and implantation site showing new bone remodeling along the edges of the implant site and complete bio-integration and replacement by trabecular bone (black asterisks).

placement[28–30,45]. Drogset et al. reported osteolysis around PLLA screws in 16% of ACLR patients[46]. Marinescu et al. reported a case of a pretibial cyst formation following the use of PLLA reinforced with HA[47].

Therefore, there remains an unmet need to overcome these inherent limitations. The present study demonstrates the safe implantation of mineral fiber-reinforced screws with the objective avoidance of such adverse degradation responses both in bone or around soft tissue. Several studies have reported that bone ingrowth promotes graft healing[11,12]. That is well reflected in the current study. The study demonstrates bone ingrowth into the implant wall at 28 W which significantly increases through 104 W. Results also demonstrate new bone formation at the implant interface occurring simultaneously with a gradual bio-integration response. Healing of the tendon graft was achieved by stable integration into the bone tunnel with graft ends conversion to new trabecular bone by 132 W. Results also demonstrate increasing scores of graft cellularity indicating graft viability and graft end integration through ossification. The high mineral content in the fiber reinforced IS, likely plays a role in this timed response. Moreover, in contrast to other added mineral compounds, such as HA and β-TCP[48], the mineral component of the bio-integrative screws is comprised of continuous fibers, built into an organized, layered structure and oriented to provide necessary biomechanical properties at the time of implantation.

Macrophages have the unique ability to perform opposing functions leading to a 'kill or repair' response. This divergent response is reflected by the existence of pro-inflammatory M1-like macrophages which differ from pro-healing M2-like macrophages[49,50].

Previously published preclinical studies for fiber reinforced implants demonstrate a similar cellular response observed in this study dominated by a non-destructive phagocytic response during polymer degradation[35,51]. The cellular response at all sites was characterized by non-inflammatory M2-like macrophages and MNGCs, with peak bioabsorption at 52 W to 104 W. Our results indicate minimal M2-like macrophages response. Suppressing adverse inflammation by stable graft fixation and early healing with reduced tendon graft-to-bone tunnel motion is crucial to the success of ACLR[52] and well demonstrated in this translational study model.

Limitations of this study include the small cohort and lack of a control group. However, this design was deliberate, and the sample size deemed sufficient for a pre-clinical study demonstrating the safety, biocompatibility, and complete bio-integration of the fiber reinforced screw.

Strengths of this study include the long-term follow-up of 132 weeks, serial MRI imaging over time allowing for the evaluation of the entire lifetime of the implant, as well as the multi-sectional histological evaluation which significantly increases sample size.

The present study demonstrates that a novel bio-integrative soft tissue implant is safe and effective when placed in bone or adjacent to a tendon graft within a bone tunnel. This new technology may enable commonly used accelerated rehabilitation programs while avoiding short- and long-term limitations observed with traditional interference screw fixation. Based on the current study results, clinical studies are planned with the aim of offering an effective alternative to graft fixation during ligament reconstruction procedures.

Data availability

Data generated or analysed during this study is included in this published article.

Received: 16 April 2024; Accepted: 9 October 2024
Published online: 09 November 2024

References

1. Straight, C. B., France, E. P., Paulos, L. E., Rosenberg, T. D. & Weiss, J. A. Soft tissue fixation to bone: A biomechanical analysis of Spiked Washers. *Am. J. Sports Med.* **22**, 339–343 (1994).
2. Cole, B., Sayegh, E., Yanke, A., Chalmers, P. N. & Frank, R. M. Fixation of soft tissue to bone: Techniques and fundamentals. *JAAOS-J. Am. Acad. Orthop. Surg.* **24**, 83–95 (2016).
3. Sanchez-Sotelo, J. Total shoulder arthroplasty. *Open. Orthop. J.* **5**, 106 (2011).
4. Martinek, V. & Friederich, N. F. Tibial and pretibial cyst formation after anterior cruciate ligament reconstruction with bioabsorbable interference screw fixation. *Arthrosc. J. Arthrosc. Relat. Surg.* **15**, 317–320 (1999).
5. Lepow, G. & Green, J. B. Reconstruction of a neglected Achilles tendon rupture with an Achilles tendon allograft: A case report. *J. Foot Ankle Surg.* **45**, 351–355 (2006).
6. Beals, T. C., Crim, J. & Nickisch, F. Deltoid ligament injuries in athletes: Techniques of repair and reconstruction. *Oper. Tech. Sports Med.* **18**, 11–17 (2010).
7. Moffat, K. L., Wang, I. N. E., Rodeo, S. A. & Lu, H. H. Orthopedic interface tissue engineering for the biological fixation of soft tissue grafts. *Clin. Sports Med.* **28**, 157–176 (2009).
8. Chen, C. H. Strategies to enhance tendon graft-bone healing in anterior cruciate ligament reconstruction. *Chang. Gung Med.* **32**, 483–493 (2009).
9. Deehan, D. J. & Cawston, T. E. The biology of intergration of the anterior cruciate ligament. *J. Bone Jt. Surg. Ser. B* **87**, 889–895 (2005).
10. West, R. & Harner, C. Graft selection in anterior cruciate ligament reconstruction. *JAAOS-J. Am. Acad. Orthop. Surg.* **13**, 197–207 (2005).
11. Chen, C. H. Graft healing in anterior cruciate ligament reconstruction. *BMC Sports Sci. Med. Rehabil.* **1**, (2009).
12. Majidinia, M., Sadeghpour, A. & Yousefi, B. The roles of signaling pathways in bone repair and regeneration. *J. Cell. Physiol.* **233**, 2937–2948 (2018).
13. Lu, H. H. & Thomopoulos, S. Functional attachment of soft tissues to bone: Development, healing, and tissue engineering. *Annu. Rev. Biomed. Eng.* **15**, 201–226 (2013).
14. Schlecht, S. Understanding entheses: Bridging the gap between clinical and anthropological perspectives. *Anat. Rec Adv. Integr. Anat. Evol. Biol.* **295**, 1239–1251 (2012).
15. Walsh, M. P., Wijdicks, C. A., Parker, J. B., Hapa, O. & LaPrade, R. F. A comparison between a retrograde interference screw, suture button, and combined fixation on the tibial side in an all-inside anterior cruciate ligament reconstruction. **37**, 160–167. https://doi.org/10.1177/0363546508323747 (2008).

16. Wanich, T., Choi, J. H. & Yocum, L. A. *Figure of 8 Technique and Outcomes. Elbow Ulnar Collateral Ligament Injury* (Springer International Publishing, 2021). https://doi.org/10.1007/978-3-030-69567-5_21.
17. Magen, H. E., Howell, S. M. & Hull, M. Structural properties of six tibial fixation methods for Anterior Cruciate Ligament Soft tissue grafts. *Am. J. Sports Med.* **27**, 35–43 (1999).
18. Barber, F. A. Biodegradable materials: Anchors and interference screws. *Sports Med. Arthrosc.* **23**, 112–117 (2015).
19. Suchenski, M. et al. Material properties and composition of soft-tissue fixation. *Arthrosc. J. Arthrosc. Relat. Surg.* **26**, 821–831 (2010).
20. Mascarenhas, R. et al. Bioabsorbable versus metallic interference screws in anterior cruciate ligament reconstruction: A systematic review of overlapping meta-analyses. *Arthrosc. J. Arthrosc. Relat. Surg.* **31**, 561–568 (2015).
21. Pandey, V., Acharya, K., Rao, S. & Rao, S. Femoral tunnel-interference screw divergence in anterior cruciate ligament reconstruction using bone-patellar tendon-bone graft: A comparison of two techniques. *Indian J. Orthop.* **45**, 255–260 (2011).
22. Sawyer, G. A., Anderson, B. C., Paller, D., Heard, W. M. R. & Fadale, P. D. Effect of interference screw fixation on ACL graft tensile strength. *J. Knee Surg.* **26**, 155–159 (2013).
23. Hughes, T. B. Bioabsorbable implants in the treatment of hand fractures: An update. *Clin. Orthop. Relat. Res.* **445**, 169–174 (2006).
24. Marinescu, R., Antoniac, I., Laptoiu, D., Antoniac, A. & Grecu, D. Complications related to biocomposite screw fixation in ACL reconstruction based on clinical experience and retrieval analysis. *Mater. Plast.* **52**, 340–344 (2015).
25. Kaeding, C., Farr, J., Kavanaugh, T. & Pedroza, A. A prospective randomized comparison of bioabsorbable and titanium anterior cruciate ligament interference screws. *Arthrosc. J. Arthrosc. Relat. Surg.* **21**, 147–151 (2005).
26. Ramos, D. M., Dhandapani, R., Subramanian, A., Sethuraman, S. & Kumbar, S. G. Clinical complications of biodegradable screws for ligament injuries. *Mater. Sci. Eng. C.* **109**, 110423 (2020).
27. Konan, S. & Haddad, F. S. A clinical review of bioabsorbable interference screws and their adverse effects in anterior cruciate ligament reconstruction surgery. *Knee.* **16**, 6–13 (2009).
28. Stener, S. et al. A long-term, prospective, randomized study comparing biodegradable and metal interference screws in anterior cruciate ligament reconstruction surgery: Radiographic results and clinical outcome. *Am. J. Sports Med.* **38**, 1598–1605 (2010).
29. Scorsato, P. S. et al. Evaluation of the degradation of two bioabsorbable interference screws: An in-vivo study in sheep. *Acta Cirúrgica Bras.* **37**, e370405 (2022).
30. Pereira, H. et al. Migration of bioabsorbable screws in ACL repair. How much do we know? A systematic review. *Knee Surg. Sport Traumatol. Arthrosc.* **21**, 986–994 (2013).
31. Frosch, K. H. et al. Magnetic resonance imaging analysis of the bioabsorbable Milagro™ interference screw for graft fixation in anterior cruciate ligament reconstruction. *Strateg. Trauma. Limb Reconstr.* **4**, 73–79 (2009).
32. Preiss-Bloom, O., Poreh, D., Merchav-Feurmann, R. & Lindner, T. *OSSIOfiber ™ Intelligent Bone Regeneration Technology Overview Introduction: Developing the Ideal Bone Fixation Material*. www.ossio.io (2019).
33. Verrier, S., Blaker, J. J., Maquet, V., Hench, L. L. & Boccaccini, A. R. PDLLA/Bioglass® composites for soft-tissue and hard-tissue engineering: An in vitro cell biology assessment. *Biomaterials* **25**, 3013–3021 (2004).
34. Hench, L. L., Splinter, R. J., Allen, W. C. & Greenlee, T. K. Bonding mechanisms at the interface of ceramic prosthetic materials. *J. Biomed. Mater. Res.* **5**, 117–141 (1971).
35. Berlet, G. C., Merchav-Feuermann, R. & Jackson, N. Bio-integration and bone fixation performance of continuous mineral fiber-reinforced implants. **5**, 2473011420S0012. https://doi.org/10.1177/247301142OS00127 (2020).
36. Rousselle, S. D., Ramot, Y., Nyska, A. & Jackson, N. D. Pathology of bioabsorbable implants in preclinical studies. *Toxicol. Pathol.* **47**, 358–378 (2019).
37. Weiler, A., Hoffmann, R. F. G., Bail, H. J., Rehm, O. & Südkamp, N. P. Tendon healing in a bone tunnel. Part II: Histologic analysis after biodegradable interference fit fixation in a model of anterior cruciate ligament reconstruction in sheep. *Arthrosc. J. Arthrosc. Relat. Surg.* **18**, 124–135 (1999).
38. Baums, M., Zelle, B., Schultz, W., Ernstberger, T. & Klinger, H. M. Intraarticular migration of a broken biodegradable interference screw after anterior cruciate ligament reconstruction. *Knee Surg. Sport Traumatol. Arthrosc.* **14**, 865–868 (2006).
39. Emond, C., Woelber, E., Kurd, S., Ciccotti, M. & Cohen, S. B. A comparison of the results of anterior cruciate ligament reconstruction using bioabsorbable versus metal interference screws: A meta-analysis. *JBJS* **93**, 572–580 (2011).
40. Debieux, P. et al. Bioabsorbable versus metallic interference screws for graft fixation in anterior cruciate ligament reconstruction. *Cochrane Database Syst. Rev.* **7**, (2016).
41. Hovis, W. & Bucholz, R. Polyglycolide bioabsorbable screws in the treatment of ankle fractures. *Foot Ankle Int.* **18**, 128–131 (1997).
42. Walton, M. & Cotton, N. J. Long-term in vivo degradation of poly-L-lactide (PLLA) in bone. *J. Biomater. Appl.* **21**, 395–411 (2007).
43. Seino, D., Fukunishi, S. & Yoshiya, S. Late foreign-body reaction to PLLA screws used for fixation of acetabular osteotomy. *J. Orthop. Traumatol.* **8**, 188–191 (2007).
44. Gonzalez-Lomas, G., Cassilly, R. T., Remotti, F. & Levine, W. N. Is the etiology of pretibial cyst formation after absorbable interference screw use related to a foreign body reaction? *Clin. Orthop. Relat. Res.* **469**, 1082–1088 (2011).
45. McGuire, D., Barber, F., Elrod, B. & LE, P. Bioabsorbable interference screws for graft fixation in anterior cruciate ligament reconstruction. *Arthrosc. J. Arthrosc. Relat. Surg.* **15**, 463–473 (1999).
46. Drogset, J. O., Grøntvedt, T. & Myhr, G. Magnetic resonance imaging analysis of bioabsorbable interference screws used for fixation of bone-patellar tendon-bone autografts in endoscopic reconstruction of the anterior cruciate ligament. *Am. J. Sports Med.* **34**, 1164–1169 (2006).
47. Marinescu, R., Laptoiu, D., Socoliuc, C. & Antoniac, I. Pretibial cyst formation in ACL reconstruction-A case report. *Key Eng. Mater.* **695**, 111–117 (2016).
48. Hayashi, K., Kishida, R., Tsuchiya, A. & Ishikawa, K. Granular honeycombs composed of Carbonate Apatite, Hydroxyapatite, and β-Tricalcium phosphate as bone graft substitutes: Effects of composition on bone formation and maturation. *ACS Appl. Bio Mater.* **3**, 1787–1795 (2020).
49. Sica, A. & Mantovani, A. Macrophage plasticity and polarization: In vivo veritas. *J. Clin. Invest.* **122**, 787–795 (2012).
50. Mantovani, A., Biswas, S. K., Galdiero, M. R., Sica, A. & Locati, M. Macrophage plasticity and polarization in tissue repair and remodelling. *J. Pathol.* **229**, 176–185 (2013).
51. Jackson, N. D., Nyska, A., Palmanovich, E. & Nyska, M. The biointegration profile of fiber-reinforced plates following tibial implantation in sheep. *J. Orthop. Res.* **42**, 360–372 (2024).
52. Yao, S., Fu, B. S. C. & Yung, P. S. H. Graft healing after anterior cruciate ligament reconstruction (ACLR). *Asia-Pacific J. Sport Med. Arthrosc. Rehabil Technol.* **25**, 8–15 (2021).

Author contributions

B.J.C. and J.T.E. conceived the experiment, J.T.E and S.R. conducted the experiment, A.N. and S.R prepared Figs. 2, 3, 4, 5 and 6. All authors analyzed the results and reviewed the manuscript.

Declarations

Competing interests

Brian J. Cole, MD, MBA: Aesculap/B.Braun: Research support American Journal of Sports Medicine: Editorial or governing board Arthrex Inc: IP royalties, paid consultant, research support Bandgrip Inc: Stock or stock options Elsevier Publishing: IP royalties, financial or material support Journal of the American Academy of Orthopedic Surgeons: Editorial or governing board JRF Ortho: Other financial or material support National Institutes of Health (NIAMS & NICHD): Research support Ossio: Stock or stock options. Abraham Nyska, DVM, Dipl. ECVP, Fellow IATP: Ossio: Paid consultant. Jeremiah T. Easley, DVM, DACVS: None. Serge Rousselle, DVM, ACVP: None.

Additional information

Correspondence and requests for materials should be addressed to B.J.C.

Reprints and permissions information is available at www.nature.com/reprints.

Publisher's note Springer Nature remains neutral with regard to jurisdictional claims in published maps and institutional affiliations.